Supplement of Atmos. Chem. Phys., 16, 2525–2541, 2016
http://www.atmos-chem-phys.net/16/2525/2016/
doi:10.5194/acp-16-2525-2016-supplement

Atmospheric Chemistry and Physics Open Access EGU

Supplement of

Light absorption and morphological properties of soot-containing aerosols observed at an East Asian outflow site, Noto Peninsula, Japan

Sayako Ueda et al.

Correspondence to: Sayako Ueda (ueda-s@stelab.nagoya-u.ac.jp) and Tomoki Nakayama (nakayama@stelab.nagoya-u.ac.jp)

S1 Collection efficiency of the ACSM

A collection efficiency (CE) of the ACSM was determined by comparing the mass concentrations of ammonium and sulfate derived by the ACSM to those measured by a conventional filter based off-line chemical analysis. The filter samples were collected using a 9-stage Andersen sampler (model AN-200, Tokyo Dylec corp.) with a flow rate of 28.3 L/min. Sampling duration was 1 week per sample. The filters were extracted and water soluble inorganic components were analyzed by ion chromatography. Ammonium and sulfate concentrations were integrated for the smallest 3 stages (including backup filter) to get the PM1.1 fraction. The CE was tuned so that the ACSM derived ammonium and sulfate match the filter based analysis.

In addition, volume concentrations of NR components were calculated using the ACSM data using the same procedure with our previous study (Nakayama et al. 2014), and were compared to volume concentrations estimated using the SMPS data (TSI, model 3936L72). As a result, the volume concentrations estimated from SMPS data were found to be about 1.7 times larger than those calculated from ACSM data. While different size-cut profiles of the ACSM, Andersen sampler, and SMPS may have affected the result, measurement uncertainty of SMPS may also contribute to the difference.

S2 Morphological types of individual particles

Based on TEM image analysis, the particles were classified into seven types based on their morphological features, as presented in Figure 8.

Particles classified as type 1 are aggregations of globules with a diameter less than 50 nm, which is characteristic of soot particles (Janzen, 1980; Pósfai et al., 2004; Murr and Soto, 2005). The results of the EDS analysis suggested that particles in this type were composed mainly of carbon.

Particles of types 2 and 3 are, respectively, single spherical and single coccoid (having parallel straight lines for the particle perimeter). These particles showed strong contrast with the film, suggesting that they are thick or highly crystalline. Because the length of the Pt/Pd shadow of these particles is long (i.e., comparable to the particle diameter), it can be inferred

that these were collected on the film as solid particles. According to results of the EDS analysis, type 2 and 3 particles were mostly sulfate-rich. Similar coccoid shaped sulfate particles have been reported by several studies on aerosols in urban regions and an Asian outflow (Li and Shao, 2010; Ueda et al., 2011), as well as aerosols emitted from biomass burning (Li et al., 2003). These workers identified such particles as ammonium sulfate particles based on selected–area electron diffraction analysis.

Type 4 particles have a spherical cap and show weak contrast to the collection film and a short Pt/Pd shadow. The short shadow length suggests a dome shape, implying that the particles were not solid when sampled. Most type 4 particles are rich in sulfur, and several of them were rich in carbon or sea-salt.

Type 5 particles are clustered, connected to form numerous spherical or coccoid units resembling type 2 or 3 particles in shape and size (0.2–0.5 μm diameter). Most type 5 particles in this study were also sulfate-rich.

Type 6 particles are crystalline coarse particles having some straight lines for the particle perimeter, but an otherwise coccoid shape. These particles have larger diameters (around 1 μm) than type 3. Most of the type 6 particles were sea salt-rich or aged sea salt-rich particles.

Type 7 particles are recrystallized droplet particles. They show a short Pt/Pd shadow, similar to type 4 particles, but partially show a strong contrast with the collection film. These results imply that they dried on the film after their collection as liquid particles. Most type 7 particles were also sea salt-rich or aged sea salt-rich.

The volume-equivalent diameters of each particle were calculated from measurements of the projected particle area *S*. For type 1, 2, 3, 5 and 6 particles, which were considered to be solid at the time of their collection, the particle diameter *d* was defined as $2(S/\pi)^{1/2}$. For types 4 and 7, which were considered as liquid droplets at the time of their collection, *d* was defined as $2^{2/3}(S/\pi)^{1/2}$ by assuming half-sphere.

S3 Mixing states of individual particles

The mixing states of particles were classified by comparing particle morphology before and after irradiation by the intense electron beam of the EDS analysis. The types of mixing states are shown in Figure 9. Type *a* is non-volatile soot particles, which have the characteristic

shape of soot (i.e., morphological type 1) and show no change in morphological appearance after irradiation by electron beam. Type *b* is non-volatile particles without the characteristic shape of soot. Type *c* is mixed particles of beam-sensitive material and non-volatile soot aggregate. Type *d* is mixed particles of beam-sensitive material and a non-volatile core, without the characteristic shape of soot. Type *e* is semi-volatile particles. Although contrasts of the type *e* particles decrease overall after irradiation by a high electron beam, the area does not change. In contrast to types *b* and *c*, type *e* particles do not have a non-volatile core. Type *f* is volatile particles.

S4 Internal mixing states and shape factors for soot-containing particles

The shape factors for soot-containing particles were estimated by electron micrographs before and after irradiation with an intense electron beam. Figure S1 shows examples of electron microphotographs of a soot-containing particle before and such irradiation together with their shape factors determined in this study. The projected area (A_p), perimeter (L_p), length of longest axis (a), right-angled length to longest axis (b), and coordinates of folding center (x_p, y_p) of soot-containing particles before EDS analysis, and the projected area (A_s) and coordinates of folding center (x_s, y_s) of soot in the particle after EDS analysis were measured using image analysis software. Using these, six parameters for soot-containing particles (particle and soot diameters (d_p and d_s), volume fraction and relative position of soot (VF_s and RP), circularity factor (CF), and aspect ratio (AR)) were estimated based on the equation shown in Table S1. The CF and AR represent shape factors; their values for a circle are 1, while for irregular shapes are less than 1 and higher than 1, respectively. The RP is an indicator of soot position in the particle. Values of 0, 1, and > 1 mean that the soot is in the center of the soot-containing particle, in a position equal to the sphere-equivalent diameter from the particle center, or outside of the sphere-equivalent diameter from the particle center, respectively.

References

Janzen, J.: Extinction of light by highly nonspherical strongly absorbing colloidal particles: spectrophotometric determination of volume distributions for carbon blacks, Appl. Opt., 19, 2977–2985, doi: 10.1364/AO.19.002977, 1980.

Li, J., Pósfai, M., Hobbs, P. V., and Buseck, P. R.: Individual aerosol particles from biomass burning in southern Africa: 2, Compositions and aging of inorganic particles, J. Geophys. Res., 108, D13, 8484, doi:10.1029/2002JD002310, 2003.

Li, W. and Shao, L.: Mixing and water-soluble characteristics of particulate organic compounds in individual urban aerosol particles, J. Geophys. Res., 115, D02301, doi:10.1029/2009JD012575, 2010.

Murr, L. E. and Soto, K. F.: A TEM study of soot, carbon nanotubes, and related fullerene nanopholyhedra in common fuel-gas combustion sources, Mater. Charact., 55, 50–65. 2005.

Nakayama, T., Ikeda, Y., Sawada, Y., Setoguchi, Y., Ogawa, S., Kawana, K., Mochida, M., Ikemori, F., Matsumoto, K., and Matsumi, Y.: Properties of light-absorbing aerosols in the Nagoya urban area, Japan, in August 2011 and January 2012: Contributions of brown carbon and lensing effect, J. Geophys. Res. Atmos., 119, 12721–12739, doi:10.1002/2014JD021744, 2014.

Pósfai, M., Gelencser, A., Simonics, R., Arato, K., Li, J., Hobbs, P. V., and Buseck, P. R.: Atmospheric tar balls: Particles from biomass and biofuel burning, J. Geophys. Res., 109, D06213, doi: 10.1029/2003JD004169, 2004.

Ueda, S., Osada, K., and Takami, A.: Morphological features of soot-containing particles internally mixed with water-soluble materials in continental outflow observed at Cape Hedo, Okinawa, Japan. J. Geophys. Res. 116, doi: 10.1029/2010JD015565, 2011.

Table S1. Parameter descriptions of soot-containing particles by image analysis.

Parameter	Symbol	Equation
Particle diameter	d_p	$d_p = 2(A_p/\pi)^{1/2}$ for type 1, 2, 3, 5 and 6 particles
		$d_p = 2^{2/3}(A_p/\pi)^{1/2}$ for type 4 and 7 particles
Soot diameter	d_s	$d_s = 2(A_s/\pi)^{1/2}$
Volume fraction of soot	VF_s	$VF_s = (d_s/d_p)^3$
Relative position of soot	RP	$RP = 2[(x_p-x_s)^2+(y_p-y_s)^2]^{1/2}/d_p$
Circularity factor	CF	$CF = 4\pi A_p/L_p^2$
Aspect ratio	AR	$AR = a/b$

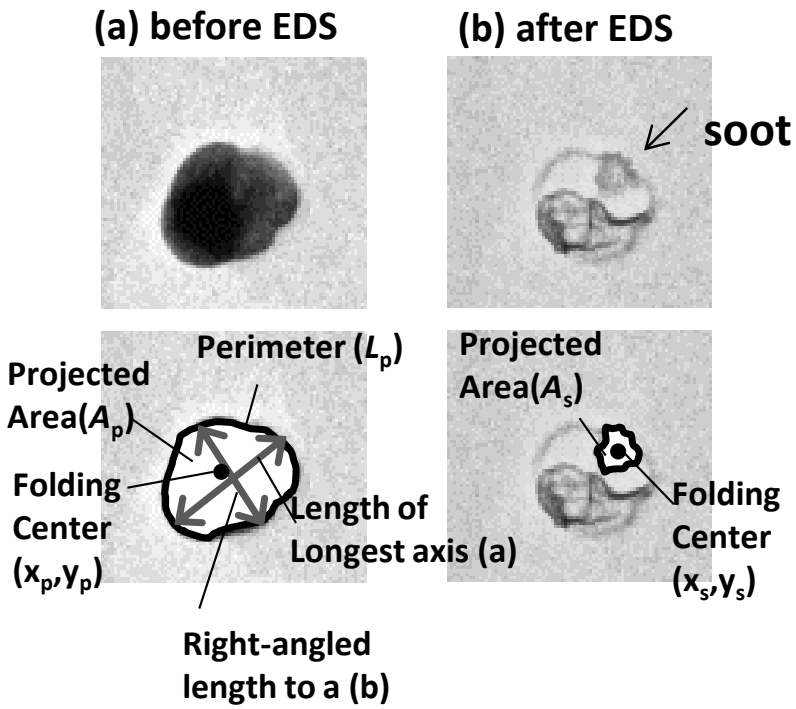

Figure S1 Photographs and shape parameters of projection area of soot-containing particles before (a) and after (b) irradiation by high densely electron beam.